# COVID-19 Report

## Modeling COVID-19 Dynamics.
## Transmission Scenarios in San Antonio, TX

**VOLUME 1**

Juan B. Gutierrez, Ph.D.

April 15, 2020

UTSA

# Contents

UTSA

# Chapter 1

# Executive Report

## 1.1 Summary

Coronavirus disease 2019 (COVID-19) is a novel human respiratory disease caused by the SARS-CoV-2 virus. The first cases of COVID-19 disease surfaced during late December 2019 in Wuhan city, the capital of Hubei province in China. Shortly after, the virus quickly spread to several countries. On January 30, 2020 The World Health Organization (WHO) declared the virus as a public health emergency of international scope. Forty one days later, on March 11, 2020 it was officially declared to be a global pandemic.

The City of San Antonio had early presence of the pathogen, although it might have not resulted in exposures for the public. San Antonio was a quarantine destination for a number of American evacuees from China and Japan. On February 7th, a plane with 91 quarantines evacuees arrived at Joint Base Lackland in San Antonio. On February 17th, two charter flights carrying passengers from Diamond Princess arrived at JBSA. These evacuees remained in quarantine for 14 days from the moment of arrival. On March 2nd, Mayor Nirenberg issued a public health emergency in the City of San Antonio. An early response prevented an explosion in the number of cases. Had the Mayor and County Judge not acted early, the crisis would have been significantly larger. The city lockdown has slowed down the progression of the disease. It allowed the health system to prepare for what is likely to be an inevitable surge.

When the first cases appeared in the US, there was no clarity about the impact of asymptomatic carriers in the dynamics of the disease. Knowledge about this matter is still evolving. However, it has become increasingly evident that COVID-19 is a highly infectious pathogen that behaves in ways very different to many other respiratory diseases.

The SARS-CoV-2 virus is a highly infectious, relentless pathogen. Once the city lockdown is lifted, a surge in cases is expected shortly after. Optimal control will be needed to minimize contagion for multiple months, until a vaccine is widely available to the public.

There is agreement between data and the mathematical model in this report. As more data becomes available, the forecast will evolve. Mathematical analysis reveals the following insights (see Figure 1.1-1):

a. **Current conditions**: 3,600 total cases. Peak by early May: 700 active cases.

b. **20% increase in mobility from now**: 8,500 total cases. Peak in mid-May: 1,500 active cases.

c. **50% increase in mobility from now**: 300,000 total cases Peak in mid-June: 48,000 active cases.

d. **Return to normal**: 920,000 total cases. Peak one month after lifting restrictions. Peak of 380,000 active cases.

NOTE: This modeling scenario uses 4/15 as the day to eliminate mobility restrictions. This model accounts for the SA Emergency Declaration

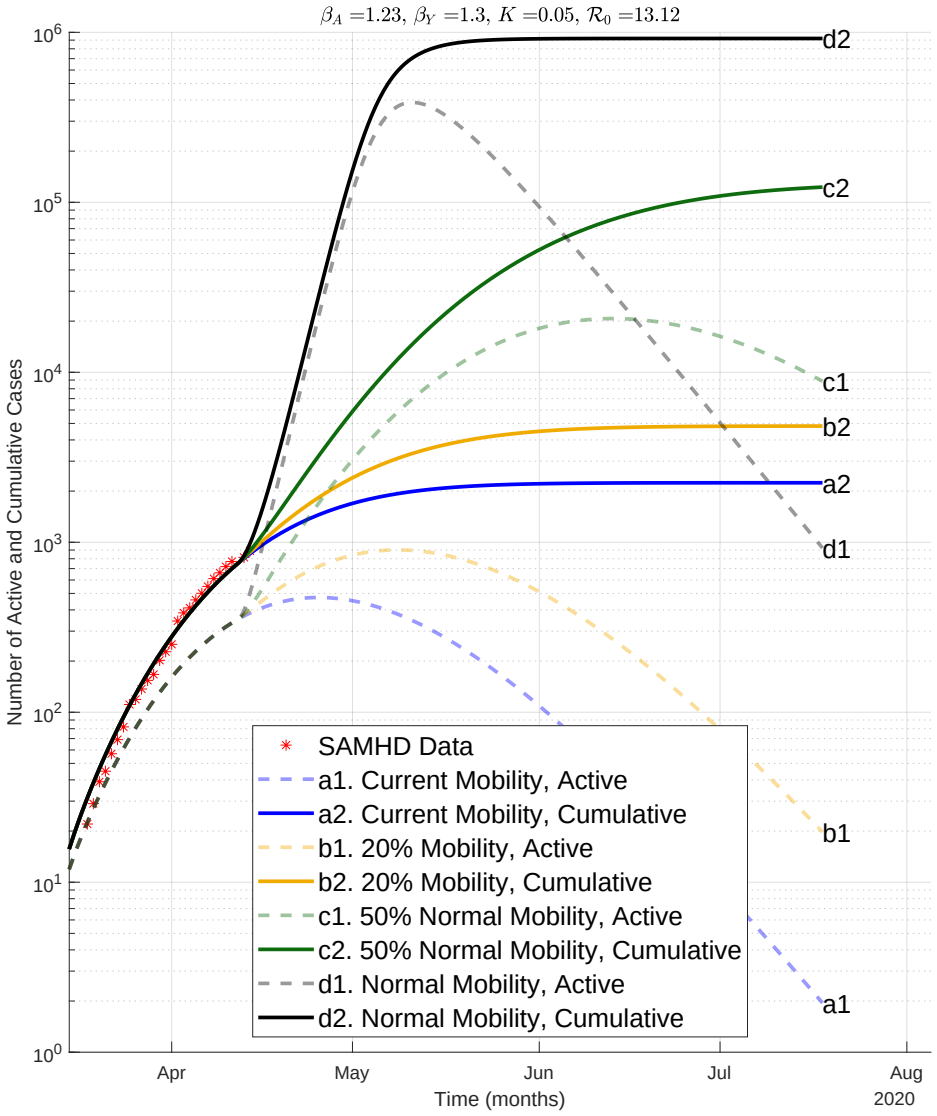


Figure 1.1-1: SanAntonio15-Apr-2020

This report contains results of mathematical modeling applied to the City of San Antonio. A Data User Agreement between UTSA, San Antonio Metropolitan Health District, and the Southwest Texas Regional Advisory Council (STRAC), facilitated secure data flow across institutional boundaries. Data is currently stored in a secured HIPAA-compliant server at UTSA, used under IRB #20-189. The chapter Technical Report contains the scientific basis for the predictions presented here. See Volume 2 to access county-level predictions of case severity and hospitalizations for every county in the US.

### 1.1.1 Data Sources

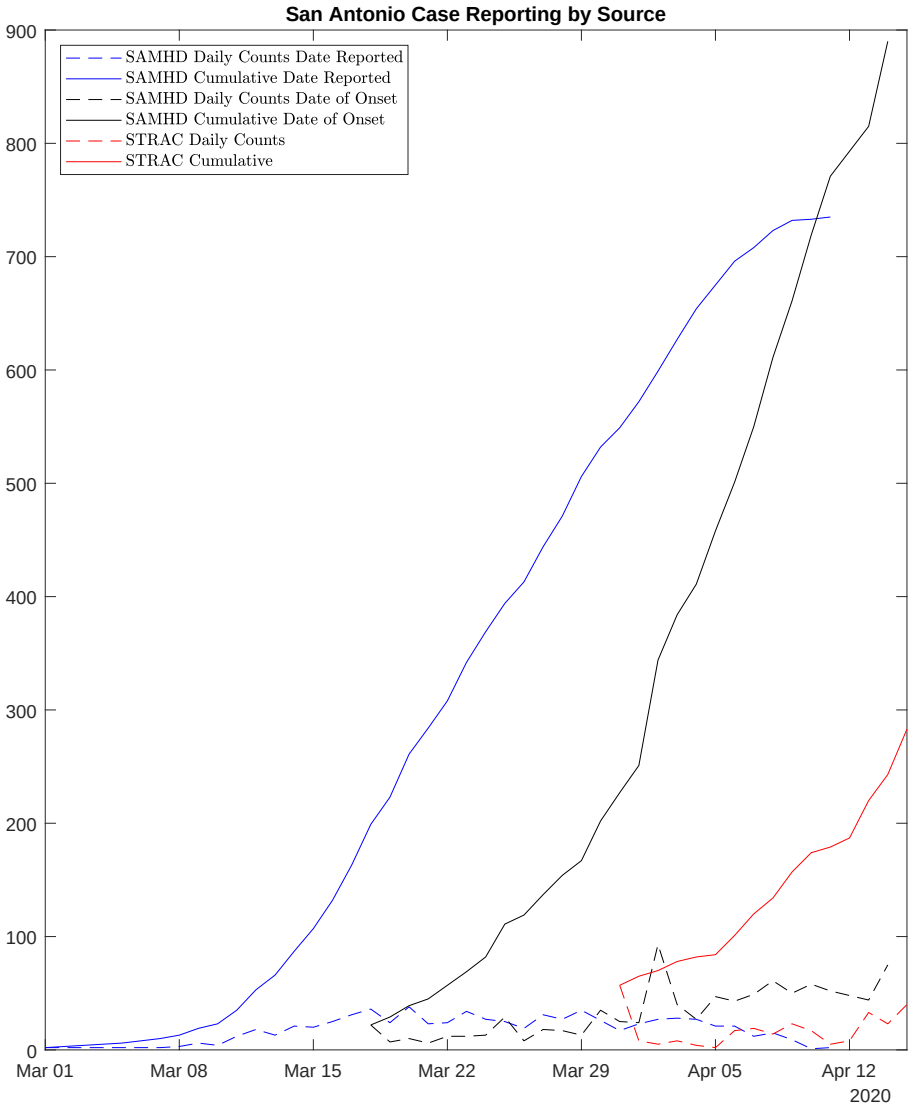


Figure 1.1-2: partnersSAMHD15-Apr-2020-Sources

### 1.1.2 Heat Maps

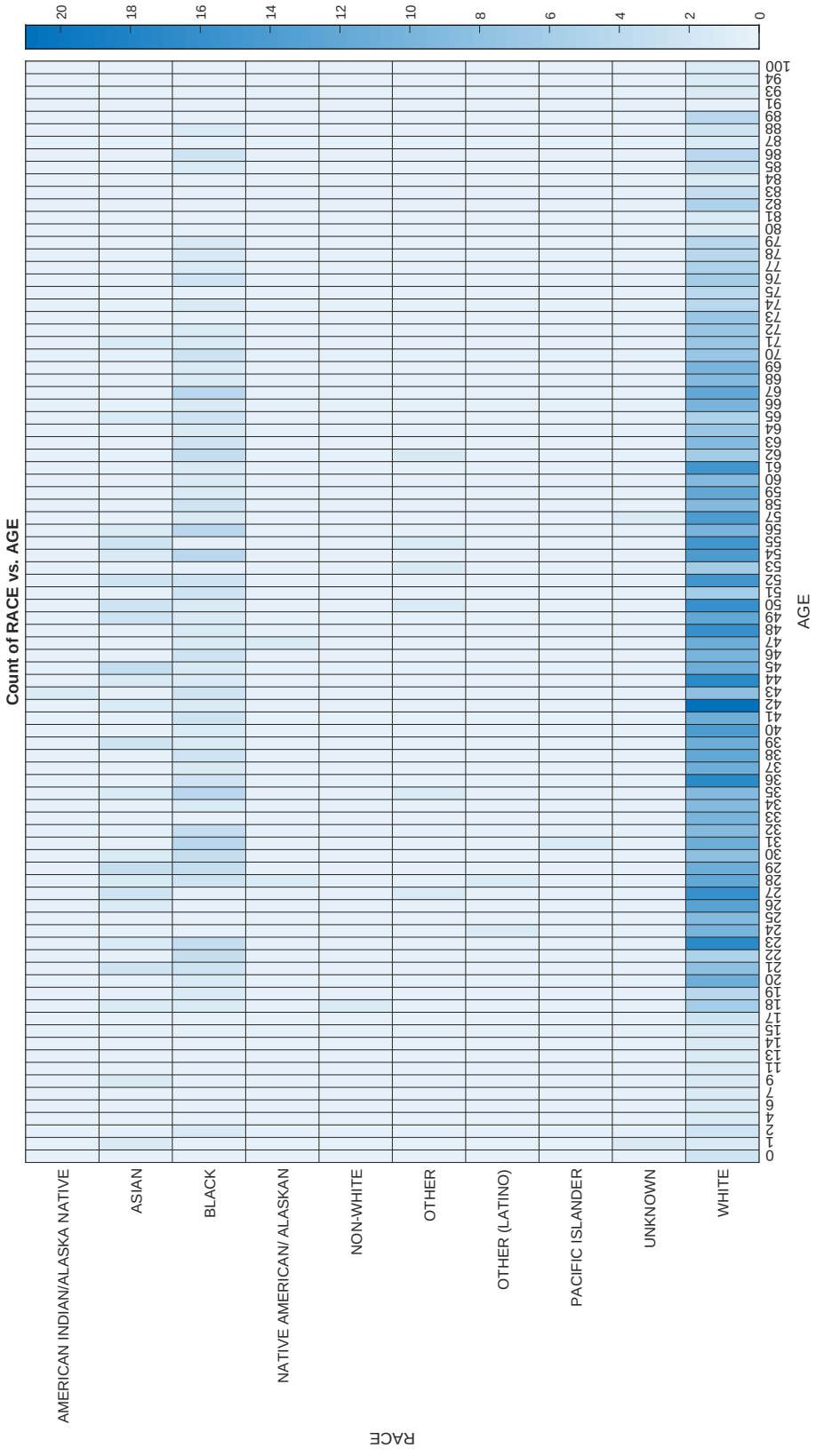


Figure 1.1-3: partnersSAMHD15-Apr-2020-HeatMapAgeRace

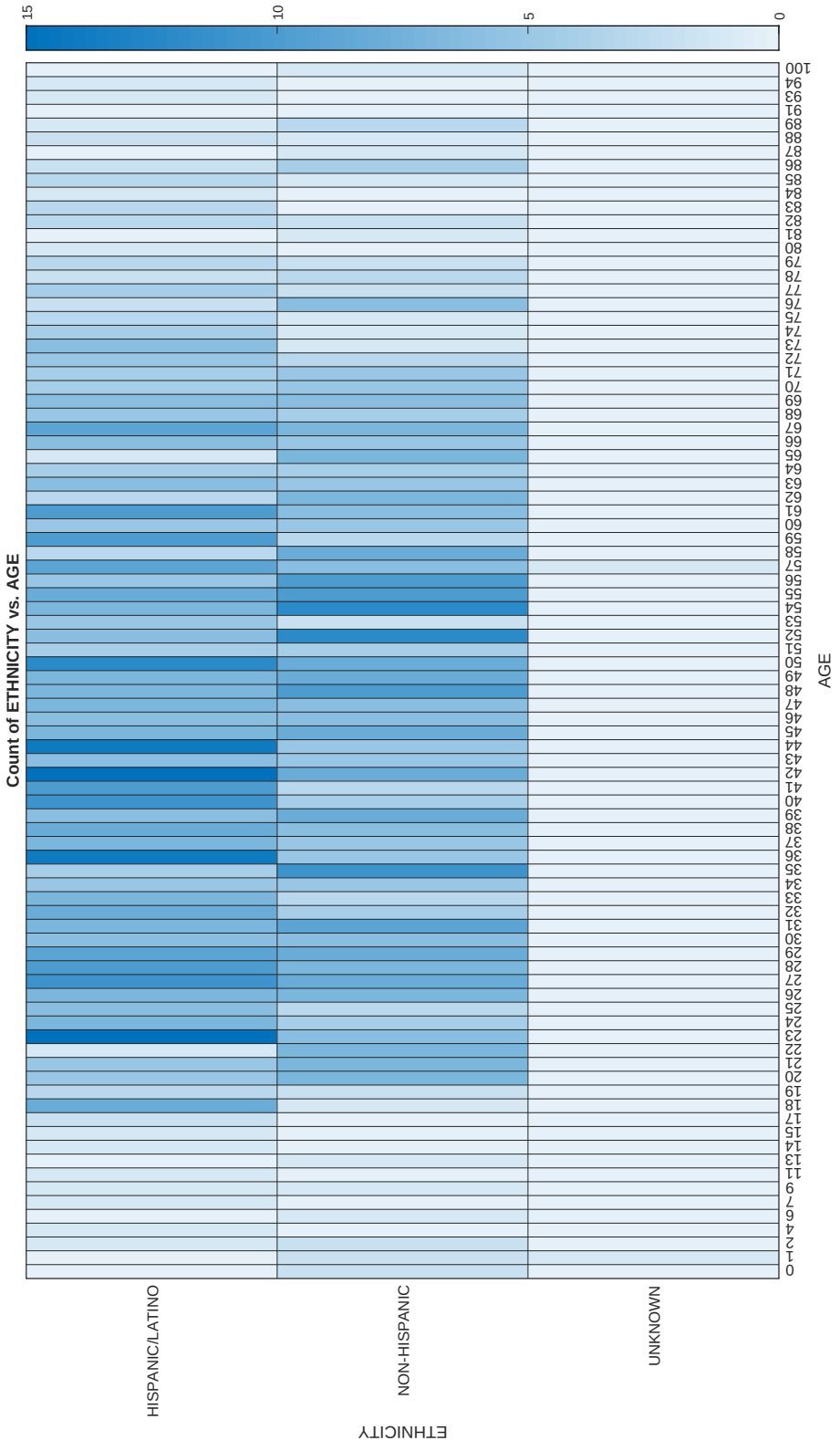


Figure 1.1-4: partnersSAMHD15-Apr-2020-HeatMapAgeEthnicity

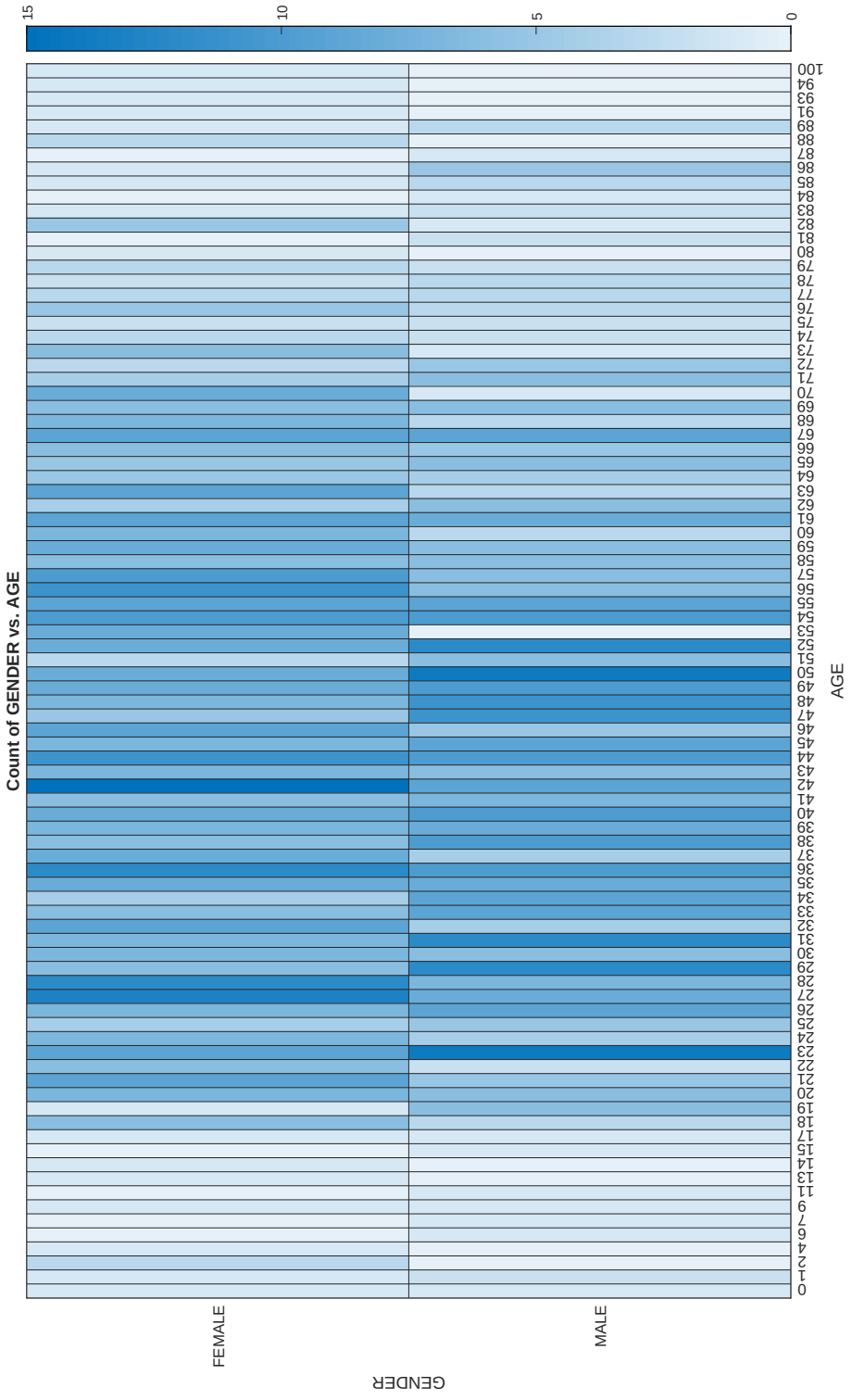


Figure 1.1-5: partnersSAMHD15-Apr-2020-HeatMapAgeGender

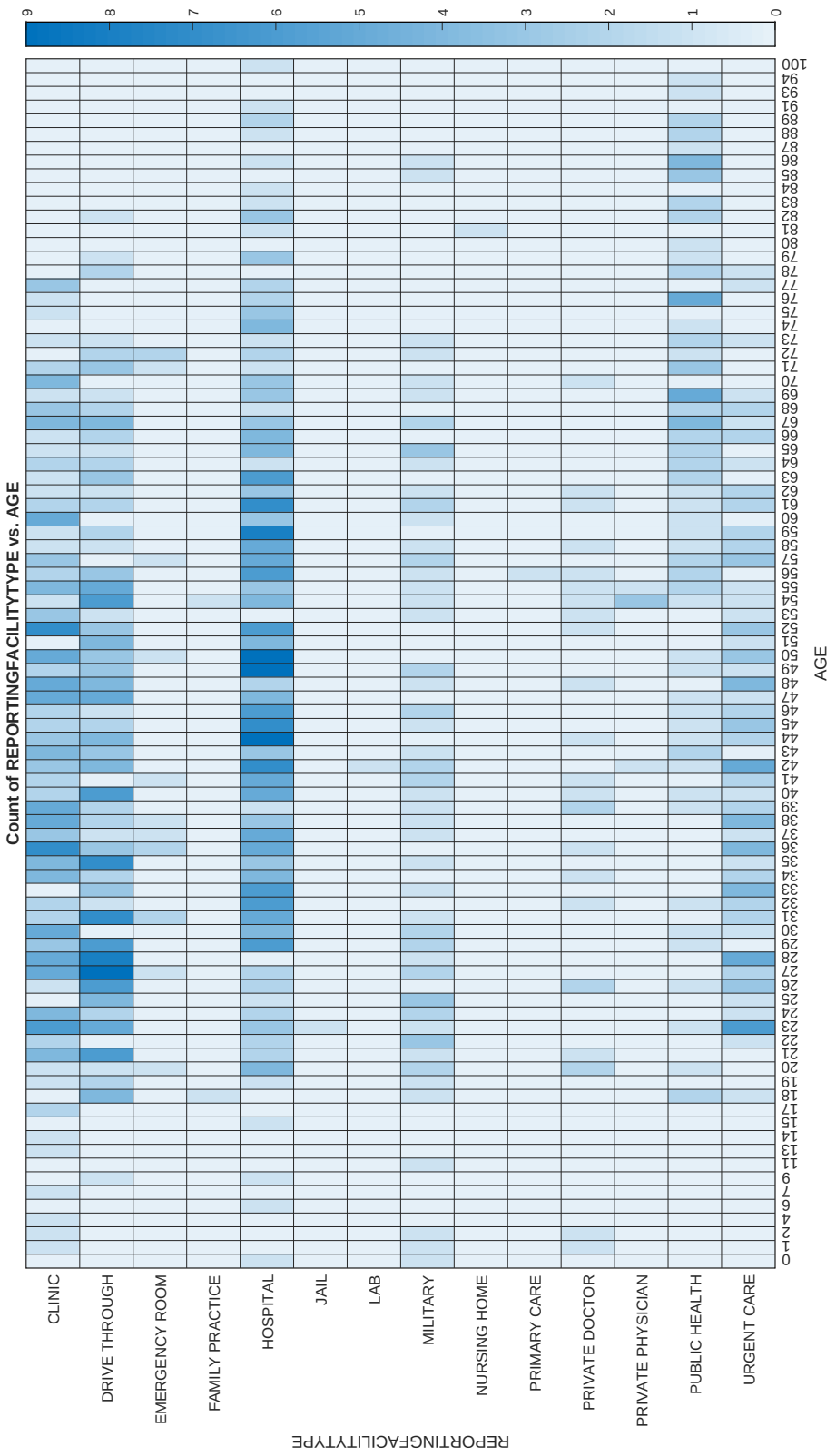


Figure 1.1-6: partnersSAMHD15-Apr-2020-HeatMapAgeFacility

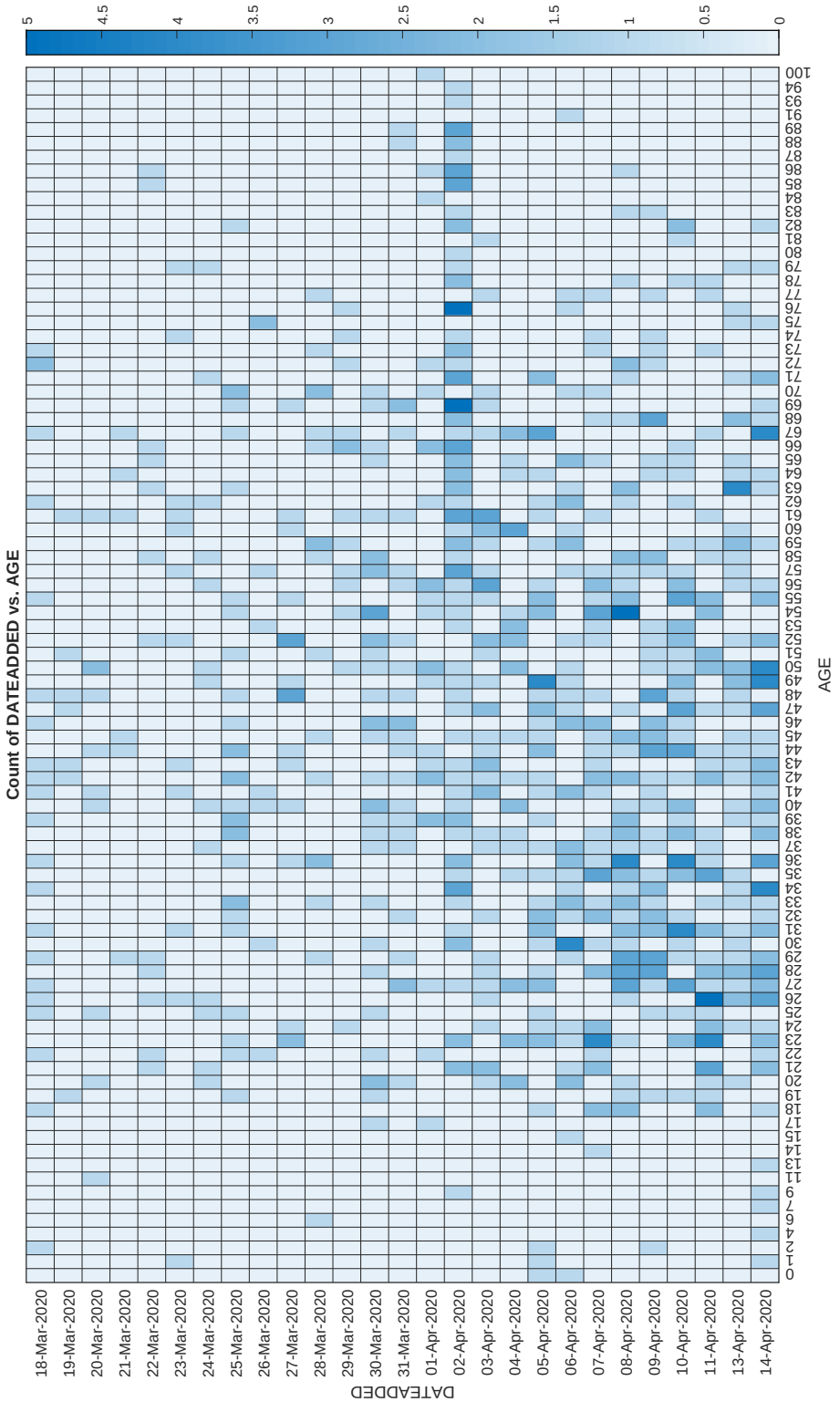


Figure 1.1-7: partnersSAMHD15-Apr-2020-HeatMapAgeDateAdded

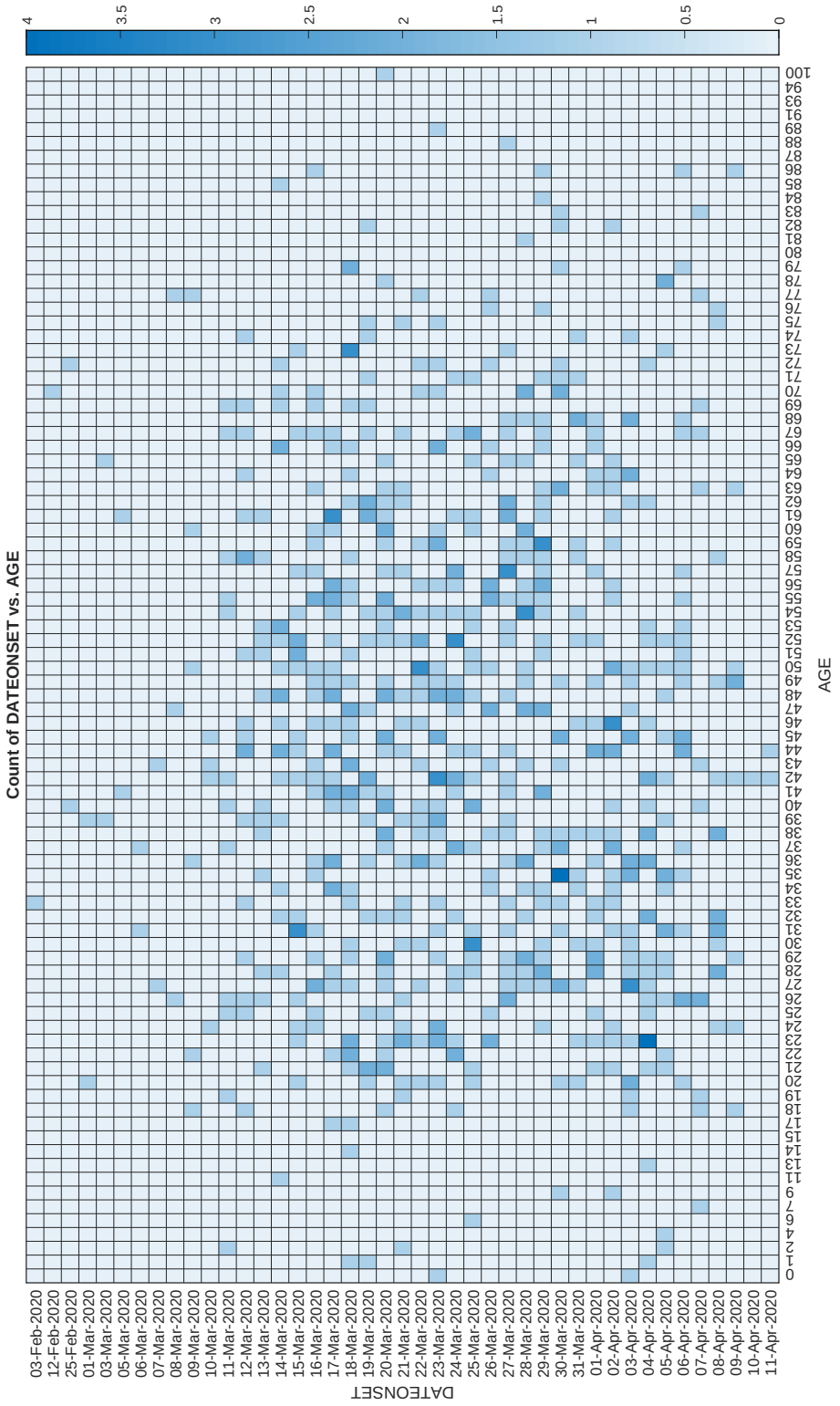


Figure 1.1-8: partnersSAMHD15-Apr-2020-HeatMapAgeDateOnset

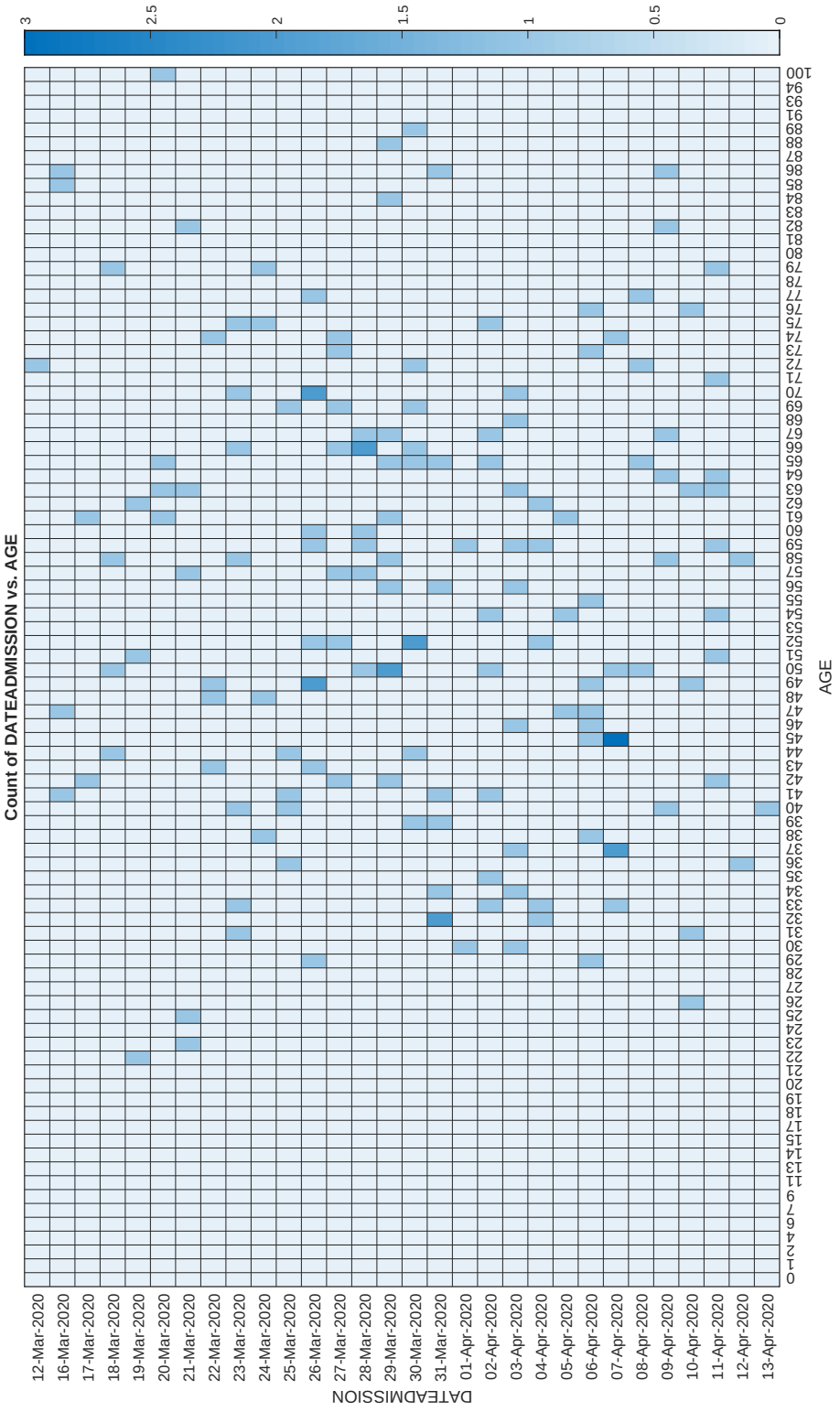


Figure 1.1-9: partnersSAMHD15-Apr-2020-HeatMapAgeDateAdmission

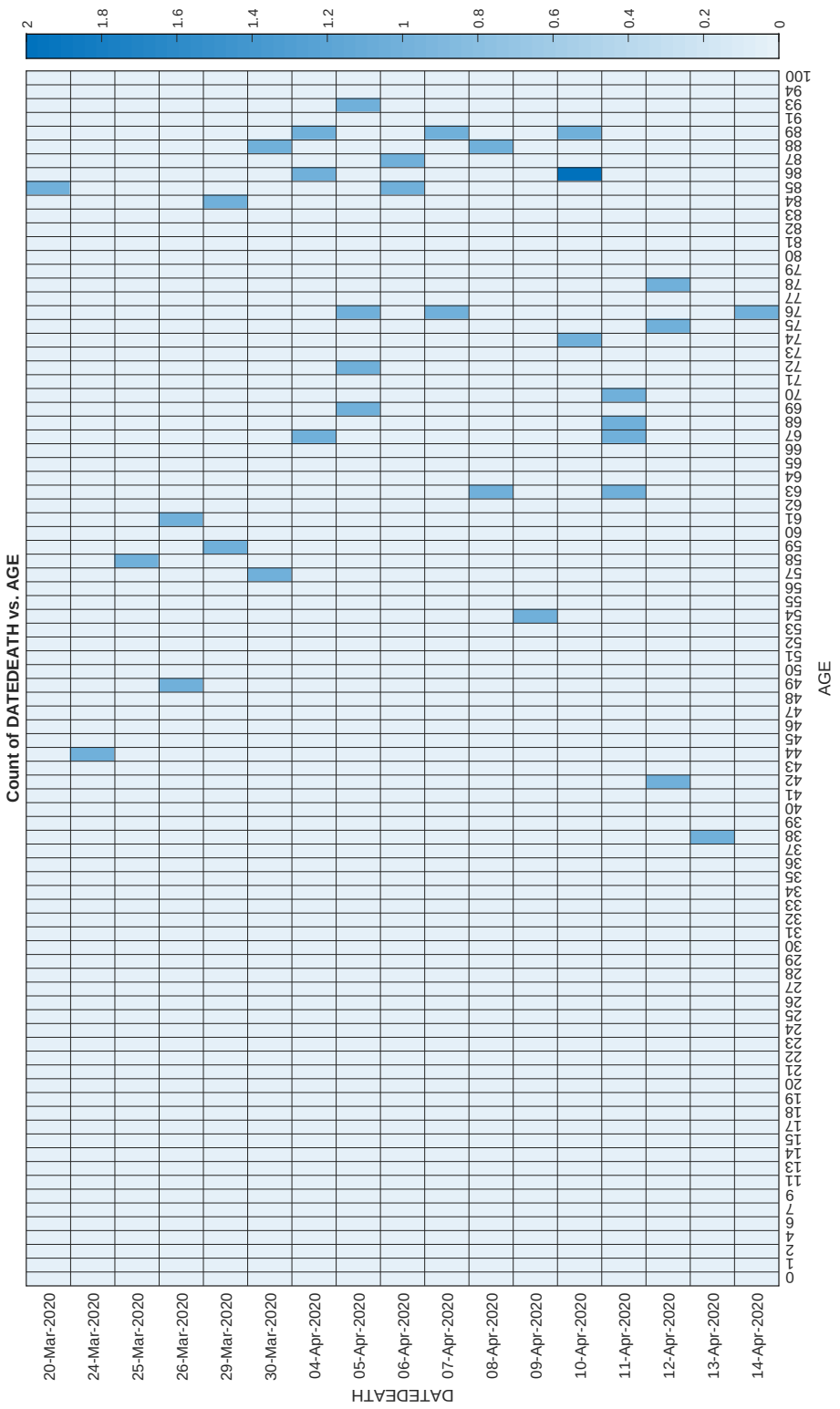


Figure 1.1-10: partnersSAMHD15-Apr-2020-HeatMapAgeDateODeath

UTSA

# Chapter 2

# Scientific Background

## 2.1 Authors

Jacob B. Aguilar[1], Ph.D.,
Jeremy Samuel Faust[2], MD MS,
Lauren M. Westafer[3], DO, MPH, MS,
Yunus Absussalam, Ph.D.[4]
Bryan Everitt[4], MD NRP
Juan B. Gutierrez[4*], Ph.D.

[1]Assistant Professor of Mathematics, Department of Mathematics and Sciences, Saint Leo University.

[2]Brigham and Women's Hospital, Department of Emergency Medicine
Division of Health Policy and Public Health, Instructor, Harvard Medical School.

[3]Assistant Professor, Department of Emergency Medicine,
University of Massachusetts Medical School-Baystate
Institute for Healthcare Delivery and Population Science.

[4]Professor of Mathematics, University of Texas at San Antonio.

[5]PGY 3, Department of Emergency Medicine, University of Texas Health San Antonio.

[*]To whom correspondence should be addressed: E-mail: juan.gutierrez3@utsa.edu.

## 2.2 Background

Coronavirus disease 2019 (COVID-19) is a novel human respiratory disease caused by the SARS-CoV-2 virus. The first cases of COVID-19 disease surfaced during late December 2019 in Wuhan city, the capital of Hubei province in China. Shortly after, the virus quickly spread to several countries [7]. On January 30, 2020 The World Health Organization (WHO) declared the virus as a public health emergency of international scope [8]. Forty one days later, on March 11, 2020 it was officially declared to be a global pandemic [9].

Asymptomatic transmission of COVID-19 has been documented [10, 11].

The viral loads of asymptomatic carriers are similar to those in symptomatic carriers [12]. A recent study concluded that asymptomatic and symptomatic carriers may have the same level of infectiousness [13]. An analysis conducted at the Los Alamos National Laboratory estimated a median $\mathcal{R}_0$ value of 5.7 (95% CI 3.8–8.9) [14]. This is a notable size difference when compared with the initial estimates of the preliminary outbreak dynamics, suggesting $\mathcal{R}_0$ to be in the interval $[0.3, 2.38]$, see [15, 16, 17, 18]. New estimations of $\mathcal{R}_0$ are surfacing as more data becomes available, however none of the estimates account for asymptomatic carriers. These findings demand a reassessment of the transmission dynamics of the COVID-19 outbreak that better account for asymptomatic transmission.

The primary aim of this manuscript is to characterize the epidemiological dynamics of SARS-CoV-2 via a compartmentalized model that takes into account asymptomatic sub-populations. The most notable result is that with the most recent data at the time of publication, COVID-19 has a large basic reproduction number $\mathcal{R}_0$ which we estimated to fall between 5.5 and 25.4, with a point estimate

of 13.2, assuming mean parameters.

## 2.3 Methods

In this section we summarize the main results, and leave mathematical calculations for the supplementary material. Numerical estimates for the basic reproduction number follow.

### 2.3.1 Dynamic Model

The *SEYAR* model for the spread of COVID-19 is formulated by decomposing the total host population ($N$) into the following five epidemiological classes: susceptible human ($S$), exposed human ($E$), symptomatic human ($Y$), asymptomatic human ($A$), and recovered human ($R$).

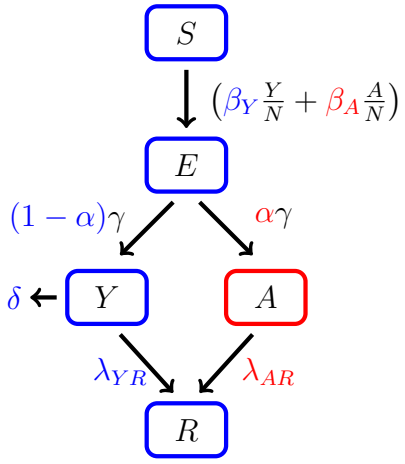


Figure 2.3-1: Schematic diagram of a COVID-19 model including an asymptomatic compartment. The arrows, except the disease-induced death ($\delta$), represent progression from one compartment to the next. Hosts progress through each compartment subject to the rates described below.

The reproduction number $\mathcal{R}_0$ is a threshold value that characterizes the local asymptotic stability of the underlying dynamical system at a disease-free equilibrium. The reproduction number arising from the dynamical system (Equation 2.2 located in the Supplemental Material) is given by

$$\boxed{\mathcal{R}_0 = (1-\alpha)\cdot\beta_Y\cdot\frac{1}{\lambda_{YR}+\delta} + \alpha\cdot\beta_A\cdot\frac{1}{\lambda_{AR}}.} \tag{2.1}$$

As the disease-induced death rate $\delta$ is of negligible size, the reproduction number $\mathcal{R}_0$ featured in Equation 2.1 above admits the following natural biological

interpretation:

$$\mathcal{R}_0 \propto \left(\begin{array}{c}\text{probability of becoming}\\ \text{symptomatic upon infection}\end{array}\right)\cdot\left(\begin{array}{c}\text{symptomatic}\\ \text{contact rate}\end{array}\right)\cdot\left(\begin{array}{c}\text{mean symptomatic}\\ \text{infectious period}\end{array}\right)$$
$$+\left(\begin{array}{c}\text{probability of becoming}\\ \text{asymptomatic upon infection}\end{array}\right)\cdot\left(\begin{array}{c}\text{asymptomatic}\\ \text{contact rate}\end{array}\right)\cdot\left(\begin{array}{c}\text{mean asymptomatic}\\ \text{infectious period}\end{array}\right).$$

A mathematical proof of the calculation yielding the reproduction number $\mathcal{R}_0$ given by Equation 2.1 is provided in the supplemental material.

The reproduction number is not a biological constant corresponding to a given pathogen [19]. In reality, the values of $\mathcal{R}_0$ fluctuate with time, and depend on numerous factors. The reproduction number $\mathcal{R}_0$ provides a way to measure the contagiousness of a disease. It is utilized by public health authorities to gauge the severity of an outbreak. The design and effective implementation of various intervention strategies are guided by estimates of $\mathcal{R}_0$. Established outbreaks will fade provided that interventions maintain $\mathcal{R}_0 < 1$.

### 2.3.2 Computation of $\mathcal{R}_0$

During the first stages of an epidemic, calculating $\mathcal{R}_0$ poses significant challenges. Evidence of this difficulty was observed in the 2009 influenza A (H1N1) virus pandemic [20]. Particularly, the COVID-19 pandemic has a different characterization in each country in which it has spread due to differences in surveillance capabilities of public health systems, socioeconomic factors, and environmental conditions.

During the initial growth of an epidemic, Anderson et al. [21] derived the following formula to determine $\mathcal{R}_0 = 1 + \frac{D \ln 2}{t_d}$, where $D$ is the duration of the infectious period, and $t_d$ is the initial doubling time. To find $t_d$, simply solve for $t$ in $Y = a_0 \cdot (1+r)^t$, where $Y = 2a_0$, and $r = 23.22\%$ (the rationale for this number is explained below). Thus, $t_d = \ln 2 / \ln(1+r) \approx 3.32$. The calculated value of the basic reproduction number using the model posed by Anderson is $\mathcal{R}_0 \approx 5.7$, using the mean value of the infectious period reported in Table 2.1. This value should be understood as an underestimation of the true $\mathcal{R}_0$ because there is no consideration of asymptomatic carriers with this formulation.

A striking characteristic of COVID-19 is the nearly perfect exponential growth reported during the first three weeks of community transmission. Figure 2.3-2 shows the number of cases reported in thirteen countries with universal health care and strong surveillance systems as of March 25, 2020. Ten of these countries are in the European zone, plus Australia, Canada and Japan. An exponential fitting for each country, conducted with the Nelder-Meade simplex algorithm [22], reveals an average coefficient of determination $R^2 = 0.9846 \pm 0.0164$. The average growth rate $r$ in the exponential model $Y = a \cdot (1+r)^t$, where $t$ is time measured in days, is $r = 23.32\%$, and the average of the initial conditions is $a = 103$ cases. Thus, the average growth of the symptomatic compartment $(Y)$ of COVID-19 during the first three weeks of community transmission in thirteen countries is characterized in average by the equation $Y = 103 \cdot 1.2332^t$. where $Y_d$ represents the distribution of time series of reported cases, and $t$ is time measured in days.

There are well known challenges in attempting to fit an exponential function to epidemiological data [23, 24, 25]. However, given the relatively slow progression of COVID-19, and the protracted infectiousness period, the growth of the symptomatic population can be well characterized by an exponential function for up to three weeks.

The parameters with the greatest uncertainty at the moment of writing are $\lambda_{YR}$ and $\lambda_{AR}$; hence, we calculated the range of $\mathcal{R}_0$ using the highest and lowest available values for these parameters. To compare the output of the model to the data from the thirteen countries studied, the growth rate found in the Equation for $Y$ above was superimposed on the model. The initial condition $a_0$ in the exponential function $Y = a_0 \cdot (1 + r)^t$ was fitted to the dynamical system with the Nelder-Meade simplex algorithm [22]. It is important to emphasize that fitting the initial value simple creates a translation of the curve. It is, therefore, remarkable that the function that describes the average behavior of the first three weeks around the world, presents a nearly perfect fit to the dynamical system using parameters that were measured in multiple settings by different groups.

Table 2.1: Values of parameters used in the average mean response plot. See Appendix for sources.

| Parameter | Description | Dimension | Value | |
|---|---|---|---|---|
| $\boxed{FITTED}$ | | | | |
| $\beta_Y$ | Effective contact rate from symptomatic to susceptible. | $days^{-1}$ | 1.30 | |
| $\beta_A$ | Effective contact rate from asymptomatic to susceptible. | $days^{-1}$ | 1.23 | |
| $\boxed{BIOLOGICAL}$ | | | | |
| $\gamma^{-1}$ | Mean latent period. | days | 5.2 | |
| $\alpha$ | Probability of becoming asymptomatic upon infection. | n/a | 0.60 | |
| $\lambda_{YR}^{-1}$ | Mean symptomatic infectious period. | $days$ | 13.5 | |
| $\lambda_{AR}^{-1}$ | Mean asymptomatic infectious period. | $days$ | 8.33 | |
| $\delta$ | Disease-induced death rate. | $days^{-1}$ | 0.026 | [26] |

## 2.4 Results

Figure 2.4-3 shows a calculation of the SEYAR model using the parameters reported in Table 2.1. This representation of the progression of the disease must be understood as a theoretical development; in reality, the progression of an epidemic depends on a multitude of factors that necessarily result in deviations from this ideal case.

Changes in behavioral patterns in response to an outbreak have an effect on the propagation of a disease. As people gain awareness of the presence of an infectious disease in their communities, a portion will take measures in order to reduce

their susceptibility. An example of this behavior corresponding to the COVID-19 pandemic is that of social distancing. Indeed, the cancellation of events likely to attract crowds, the closing of schools, and working from home will have a drastic impact on the size of the susceptible population at any given time. Figure 2.4-3 shows time series corresponding to the upper and lower estimations of the basic reproduction number, along with intervention simulations for each scenario. Figure 2.4-4 shows the variation of $\mathcal{R}_0$ with respect to the symptomatic and asymptomatic mean infectious periods, $\lambda_{YR}^{-1}$ and $\lambda_{AR}^{-1}$.

The size of the COVID-19 reproduction number documented in literature is relatively small. Our estimates indicate that $\mathcal{R}_0$ is likely to be in the interval from 5.5 to 25.4 with a point estimate of 13.2, when the asymptomatic sub-population is accounted for.

## 2.5 Discussion

The calculation of $\mathcal{R}_0$ poses significant challenges during the first stages of any outbreak, including the COVID-19 pandemic. This is due to paucity and timing of surveillance data, different methodological approaches to data collection, and different guidelines for testing. Estimates vary greatly: 0.3 [15], 2.28 [16], 2.38 [17], 3.28 [18], and others. However, none of the previous studies take into consideration the possibility of asymptomatic carriers.

The time series of symptomatic individuals provided by the SEYAR model can inform the likely progression of the disease. The compartment $Y$ must be considered as an upper bound for the progression of the COVID-19 pandemic, that is, what surveillance systems could observe in absence of public health interventions and behavior modification. However, as the COVID-19 pandemic evolves, governments around the world are taking drastic steps to limit community spread. This will necessarily dampen the growth of the disease. The SEYAR model captured faithfully the first stages of the pandemic, and remains a stark reminder of what the cost of inaction could be. It can be used as a tool to explore multiple scenarios corresponding to different interventions.

A scenario where $\mathcal{R}_0 \approx 3$ is remotely plausible requires unrealistic values for the infectious periods. If we consider the median of the other parameters to be correct, then the mean infectious periods should be approximately 4.4 days. If we reduced the probability of becoming asymptomatic upon infection to $\alpha = 0.3$, then the mean infectious periods would be 3.1 days. These infectious periods are not consistent with evidence. The necessary conclusion is that via a computational *reductio ad absurdum*, in tandem with the information we have today, $\mathcal{R}_0$ cannot be near 3.

## 2.6 Conclusion

It is unlikely that a pathogen that blankets the planet in three months can have a basic reproduction number in the vicinity of 3, as reported in the literature [1, 2, 3, 4, 5, 6]. In juxtaposition to the SARS-CoV epidemic of 2003 [27], where

only symptomatic individuals were capable of transmitting the disease, asymptomatic carriers of the SARS-CoV-2 virus may be capable of the same degree of transmission as symptomatic individuals [12]. In a public health context, the silent threat posed by the presence of asymptomatic and other undocumented carriers in the population renders the COVID-19 pandemic far more difficult to control. SARS-CoV-2 is evidently among the more contagious pathogens known, a phenomenon most likely driven by the asymptomatic sub-population.

The value of $\mathcal{R}_0$ must be understood as a threshold parameter that can be utilized to characterize disease spread. The estimations of $\mathcal{R}_0$ are expected to vary substantially per locality depending on how public health officials communicate the risk to the general public, general beliefs and (dis)information available to the population, and other socioeconomic and environmental factors affecting contact rates. Our goal with this investigation was to develop the SEYAR mean field estimate, which can be applied to different locations to provide a measure of the potential impact of the disease.

This study shows that asymptomatic individuals are major drivers for the growth of the COVID-19 pandemic. The value of $\mathcal{R}_0$ we calculated is at least double and up to one order of magnitude larger than the estimates that have been communicated in the literature and to policymakers up to this point.

## 2.7 Supplemental Material

Table 2.2: Latent period

| Parameter | Dimension | Biological | Computational | Source |
|---|---|---|---|---|
| $\gamma^{-1}$ | days | $5.1(4.5, 5.8)$ | n/a | [28] |
| | | $5.2(4.1, 7)$ | n/a | [29] |
| | | $6.4(5.6, 7.7)$ | n/a | [30] |
| | | $5.2(1.8, 12.4)$ | n/a | [31] |
| | | $5.2(4.2, 6)$ | n/a | [32] |
| | | 3.9 | n/a | [33] |
| | | $5(4.2, 6.0)$ | n/a | [34][1] |
| | | $5.6(5, 6.3)$ | n/a | [34][2] |
| | | n/a | $4.2(3.5, 5.1)$ | [14][6] |
| | | n/a | 1.25 | [35] |
| | | n/a | $3.68(3.48, 3.90)$ | [36][3] |
| | | n/a | $3.62(3.44, 3.87)$ | [36][4] |
| | | n/a | $3.43(3.30, 3.63)$ | [36][5] |
| | **Mean** | 5.2 | 3.2 | |
| | **Variance** | 0.5 | 1.3 | |

The latent period is defined to be the number of days elapsed between exposure to the pathogen and when symptoms are manifested. This parameter is also referred to as the mean incubation period in the literature. Quantities are listed as values, ranges or Median(95% CIs).

(1) This data corresponds to the case of excluding Wuhan.

(2) This data corresponds to the case of including Wuhan.

(3) This estimate corresponds to the best-fit model posterior estimates of key epidemiological parameters for simulation during January 10-23, 2020.

(4) This estimate corresponds to the best-fit model posterior estimates of key epidemiological parameters for simulation during January 24-February 3, 2020.

(5) This estimate corresponds to the best-fit model posterior estimates of key epidemiological parameters for simulation during January 24-February 8, 2020.

(6) This estimate was obtained utilizing a uniform distribution from 2.2 to 6 days.

Table 2.3: Asymptomatic Proportion

| Parameter | Dimension | Biological | Computational | Source |
|---|---|---|---|---|
| $\alpha$ | n/a | $17.9\%(15.5\%, 20.2\%)$ | n/a | [10] |
| | | $33.\bar{3}\%$ | n/a | [37][1] |
| | | $[50\%, 75\%]$ | n/a | [38] |
| | | $80\%$ | n/a | [39] |
| | | n/a | $41.6\%(16.7\%, 66.7\%)$ | [40][2] |
| | | $[80\%, 95\%]$ | n/a | [41][1] |
| | | n/a | $86\%(82\%, 90\%)$ | [36] |
| | | $78\%$ | n/a | [42] |
| | **Mean** | $60\%$ | $60\%$ | |
| | **Variance** | $10\%$ | $10\%$ | |

The probability of becoming asymptomatic upon infection is obtained by the proportion of asymptomatic infections in a given population and is utilized as a transmission factor accounting for the asymptomatic sub-population. Quantities are listed as values, ranges or Median(95% CIs).

(1) This percentage was assumed.

(2) A Bayes theorem was utilized to obtain this estimation.

Table 2.4: Asymptomatic Infectious Period

| Parameter | Dimension | Biological | Computational | Source |
|---|---|---|---|---|
| $\lambda_{AR}^{-1}$ | days | 8.33 | n/a | [43][1] |
| | | n/a | $3.45(3.24, 3.70)$ | [36][2] |

The asymptomatic infectious period is defined to the the number of days an individual who never develops symptoms exhibits viral shedding. For the asymptomatic infectious period we assumed viral shedding was synonymous with transmissibility. Quantities are listed as values, ranges or Median(95% CIs).

(1) This quantity was estimated by taking the average number of days for which viral RNA was detected via swab one day prior to the limit of quantification.

(2) This estimate corresponds to the best-fit model posterior estimates of key epidemiological parameters for simulation during January 10-23, 2020.

Table 2.5: Symptomatic Infectious Period

| Parameter | Dimension | Biological | Computational | Source |
|---|---|---|---|---|
| $\lambda_{YR}^{-1}$ | days | $[10, 11]$ | n/a | $[43]^1$ |
| | | n/a | 2.9 | [44] |
| | | $20(17, 24)$ | n/a | $[45]^2$ |
| | | 10 | n/a | [46] |
| | | n/a | $3.47(3.26, 3.67)$ | $[36]^3$ |
| | | n/a | $3.15(2.62, 3.71)$ | $[36]^4$ |
| | | n/a | $3.32(2.92, 4.04)$ | $[36]^5$ |
| | | n/a | $[4, 14]$ | $[14]^6$ |
| | **Mean** | 13.5 | 4.4 | |
| | **Variance** | 31.8 | 6.7 | |

The symptomatic infectious period is the number of days an individual who develops COVID-19 symptoms exhibits viral shedding. For the symptomatic infectious period we assumed viral shedding was synonymous with transmissibility. Quantities are listed as values, ranges or Median(95% CIs).

(1) This assumption is based on the finding that sputum viral loads showed a late and high peak around days 10 to 11.

(2) In this finding, the median duration of viral shedding was 20 days with interquartile range of $(17, 24)$.

(3) This estimate corresponds to the best-fit model posterior estimates of key epidemiological parameters for simulation during January 10-23, 2020.

(4) This estimate corresponds to the best-fit model posterior estimates of key epidemiological parameters for simulation during January 24-February 3, 2020.

(5) This estimate corresponds to the best-fit model posterior estimates of key epidemiological parameters for simulation during January 24-February 8, 2020.

(6) This interval corresponds to the range of a uniform distribution.

Equation 2.2 is a $SEYAR$ dynamical system describing the dynamics of COVID-19 transmission in a human population. The dynamical system given by Equation 2.2 was computed with the values appearing in Table 1.

$$\begin{cases} \dot{S} = -\left(\beta_Y \frac{Y}{N} + \beta_A \frac{A}{N}\right) S, \\ \dot{E} = \left(\beta_Y \frac{Y}{N} + \beta_A \frac{A}{N}\right) S - \gamma E, \\ \dot{Y} = \gamma(1-\alpha)E - (\delta + \lambda_{YR})\, Y, \\ \dot{A} = \gamma\alpha E - \lambda_{AR} A, \\ \dot{R} = \lambda_{AR} A + \lambda_{YR} Y, \end{cases} \tag{2.2}$$

where, $N = S + E + Y + A + R$. A slightly generalized model is covered below in which the model utilized in this manuscript is a specific case. The generalized $SEYAR$ dynamical system in Equation 2.3 which falls into the class of models covered by Aguilar and Gutierrez (2020) [47], (see Figure 2.7-5) is given by the

following equations:

$$\begin{cases} \dot{S} = \Lambda + \lambda_{RS} R - \left(\beta_Y \frac{Y}{N} + \beta_A \frac{A}{N} + \xi\right) S, \\ \dot{E} = \left(\beta_Y \frac{Y}{N} + \beta_A \frac{A}{N}\right) S - (\gamma + \xi) E, \\ \dot{Y} = \gamma(1-\alpha) E - (\xi + \delta + \lambda_{YR}) Y + \lambda_{AY} A, \\ \dot{A} = \gamma\alpha E - (\lambda_{AR} + \lambda_{AY} + \xi) A, \\ \dot{R} = \lambda_{AR} A + \lambda_{YR} Y - (\lambda_{RS} + \xi) R, \end{cases} \tag{2.3}$$

where, $N = S + E + Y + A + R$. The demographic parameters $\Lambda$ and $\xi$ denote the human recruitment and mortality rates, respectively. While $\lambda_{AY}$ and $\lambda_{RS}$ are the asymptomatic to symptomatic transition and relapse rates, respectively.

It is worth mentioning that for a basic $SEIR$ model, where there is only one infected compartment, the progression rate from the susceptible to the exposed class $\lambda_{SE}$ is equal to the product of the effective contact rate $\beta$ and the proportion of infected individuals $\frac{I}{N}$, so that

$$\lambda_{SE} = \beta \frac{I}{N}.$$

In our model, we decompose the infected compartment into symptomatic and asymptomatic sub-compartments. Due to this decomposition, the progression rate is given by the weighted sum

$$\lambda_{SE} = \left(\beta_Y \frac{Y}{N} + \beta_A \frac{A}{N}\right).$$

Disease-Free Equilibrium (DFE) points are solutions of a dynamical system corresponding to the case where no disease is present in the population.

**Lemma 1.** *(Reproduction Number for the SEYAR COVID-19 Model). Define the following quantity*

$$\mathcal{R}_0 := \frac{\gamma}{\gamma + \xi} \left( \frac{\beta_Y}{\delta + \lambda_{YR} + \xi} \left( \frac{\alpha \lambda_{AY}}{\lambda_{AR} + \lambda_{AY} + \xi} - (\alpha - 1) \right) + \frac{\alpha \beta_A}{\lambda_{AR} + \lambda_{AY} + \xi} \right). \tag{2.4}$$

*Then, the DFE $\mathbf{w}^\star$ for the SEYAR model in Equation 2.3 is locally asymptotically stable provided that $\mathcal{R}_0 < 1$ and unstable if $\mathcal{R}_0 > 1$.*

*Proof.* We order the compartments so that the first four correspond to the infected sub-populations and denote $\mathbf{w} = (E, Y, A, R, S)^T$. The corresponding DFE is

$$\mathbf{w}^\star = \left(0, 0, 0, 0, \frac{\Lambda}{\xi}\right)^T.$$

Utilizing the next generation method developed by Van den Driessche and Watmough [48], system in Equation 2.3 is rewritten in the following form

$$\dot{\mathbf{w}} = \Phi(\mathbf{w}) = \mathcal{F}(\mathbf{w}) - \mathcal{V}(\mathbf{w}),$$

where $\mathcal{F} := (\mathcal{F}_1, \ldots, \mathcal{F}_5)^T$ and $\mathcal{V} := (\mathcal{V}_1, \ldots, \mathcal{V}_5)^T$, or more explicitly

$$\begin{pmatrix} \dot{E} \\ \dot{Y} \\ \dot{A} \\ \dot{R} \\ \dot{S} \end{pmatrix} = \begin{pmatrix} \left(\beta_Y \frac{Y}{N} + \beta_A \frac{A}{N}\right) S \\ 0 \\ 0 \\ 0 \\ 0 \end{pmatrix} - \begin{pmatrix} (\gamma + \xi) E \\ -\gamma (1 - \alpha) E + (\xi + \delta + \lambda_{YR}) Y - \lambda_{AY} A \\ -\gamma \alpha E + (\lambda_{AR} + \lambda_{AY} + \xi) A \\ -\lambda_{AR} A - \lambda_{YR} Y + (\lambda_{RS} + \xi) R \\ -\Lambda - \lambda_{RS} R + \left(\beta_Y \frac{Y}{N} + \beta_A \frac{A}{N} + \xi\right) S \end{pmatrix}.$$

The matrix $\mathcal{V}$ admits the decomposition $\mathcal{V} = \mathcal{V}^- - \mathcal{V}^+$, where the component-wise definition is inherited. In a biological context, $\mathcal{F}_i$ is the rate of appearance of new infections in compartment $i$, $\mathcal{V}_i^+$ stands for the rate of transfer of individuals into compartment $i$ by any other means and $\mathcal{V}_i^-$ is the rate of transfer of individuals out of compartment $i$. Now, let $F$ and $V$ be the following sub-matrices of the Jacobian of the above system, evaluated at the solution $\mathbf{w}^\star$

$$F = \left(\frac{\partial \mathcal{F}_i}{\partial x_j}\bigg|_{\mathbf{w}^\star}\right)_{1 \le i,j \le 3} = \begin{pmatrix} 0 & \beta_Y & \beta_A \\ 0 & 0 & 0 \\ 0 & 0 & 0 \end{pmatrix}$$

and

$$V = \left(\frac{\partial \mathcal{V}_i}{\partial x_j}\bigg|_{\mathbf{w}^\star}\right)_{1 \le i,j \le 3} = \begin{pmatrix} (\gamma + \xi) & 0 & 0 \\ \gamma (\alpha - 1) & (\xi + \delta + \lambda_{YR}) & -\lambda_{AY} \\ -\gamma\alpha & 0 & (\lambda_{AR} + \lambda_{AY} + \xi) \end{pmatrix}.$$

A direct calculation shows that

$$V^{-1} = \begin{pmatrix} (\gamma + \xi)^{-1} & 0 & 0 \\ -\frac{\gamma((\alpha-1)(\lambda_{AR}+\xi)-\lambda_{AY})}{(\gamma+\xi)(\xi+\delta+\lambda_{YR})(\xi+\lambda_{AY}+\lambda_{AR})} & (\xi + \delta + \lambda_{YR})^{-1} & \lambda_{AY} \left((\xi + \delta + \lambda_{YR}) (\xi + \lambda_{AY} + \lambda_{AR})\right)^{-1} \\ \gamma\alpha \left((\gamma + \xi) (\lambda_{AR} + \lambda_{AY} + \xi)\right)^{-1} & 0 & (\lambda_{AR} + \lambda_{AY} + \xi)^{-1} \end{pmatrix}$$

and $FV^{-1}$ is given by the following matrix

$$\begin{pmatrix} \frac{\gamma}{(\gamma+\xi)(\lambda_{AR}+\lambda_{AY}+\xi)} \left(-\frac{\beta_Y((\alpha-1)(\lambda_{AR}+\xi)-\lambda_{AY})}{\delta+\lambda_{YR}+\xi} + \beta_A \alpha\right) & \beta_Y (\delta + \lambda_{YR} + \xi)^{-1} & \frac{1}{\lambda_{AR}+\lambda_{AY}+\xi} \left(\frac{\beta_Y \lambda_{AY}}{\delta+\lambda_{YR}+\xi} + \beta_A\right) \\ 0 & 0 & 0 \\ 0 & 0 & 0 \end{pmatrix}.$$

Let $\mathcal{I}$ denote the $3 \times 3$ identity matrix, so that the characteristic polynomial $P(\lambda)$ of the matrix $FV^{-1}$ is given by

$$\begin{aligned} P(\lambda) &= \det\left(FV^{-1} - \lambda\mathcal{I}\right), \\ &= \lambda^2 \left(\lambda - \left(\frac{\gamma\beta_Y}{(\gamma + \xi)(\delta + \lambda_{YR} + \xi)} \left(\frac{\alpha\lambda_{AY}}{\lambda_{AR} + \lambda_{AY} + \xi} + 1 - \alpha\right) + \frac{\gamma\alpha\beta_A}{(\gamma + \xi)(\lambda_{AR} + \lambda_{AY} + \xi)}\right)\right). \end{aligned}$$

The solution set $\{\lambda_i\}_{1 \le i \le 3}$ is given by

$$\left\{0, 0, \frac{\gamma\beta_Y}{(\gamma + \xi)(\delta + \lambda_{YR} + \xi)} \left(\frac{\alpha\lambda_{AY}}{\lambda_{AR} + \lambda_{AY} + \xi} + 1 - \alpha\right) + \frac{\gamma\alpha\beta_A}{(\gamma + \xi)(\lambda_{AR} + \lambda_{AY} + \xi)}\right\}.$$

Therefore, the reproduction number for the *SEYAR* model in Equation 2.3 is given by

$$\begin{aligned}\mathcal{R}_0 &:= \rho\left(FV^{-1}\right), \\ &= \max_{1\leq i\leq 3}\{\lambda_i\}, \\ &= \frac{\gamma\beta_Y}{(\gamma+\xi)(\delta+\lambda_{YR}+\xi)}\left(\frac{\alpha\lambda_{AY}}{\lambda_{AR}+\lambda_{AY}+\xi}+1-\alpha\right)+\frac{\gamma\alpha\beta_A}{(\gamma+\xi)(\lambda_{AR}+\lambda_{AY}+\xi)}, \\ &= \frac{\gamma}{\gamma+\xi}\left(\frac{\beta_Y}{\delta+\lambda_{YR}+\xi}\left(\frac{\alpha\lambda_{AY}}{\lambda_{AR}+\lambda_{AY}+\xi}-(\alpha-1)\right)+\frac{\alpha\beta_A}{\lambda_{AR}+\lambda_{AY}+\xi}\right).\end{aligned}$$

The proof of the lemma regarding the local asymptotic stability of the DFE $\mathbf{w}^\star$ corresponding to the *SEYAR* model in Equation 2.3 is now complete after invoking Theorem 2 reported by Van den Driessche and Watmough (2002) [48]. □

Equation 1 in the manuscript corresponds to the DFE solution given by $\mathbf{v}^\star = (0,0,0,0,S_0)^T$ and the absence of demographic parameters and asymptomatic to symptomatic transition rate. It can alternatively be obtained by letting $\xi = \lambda_{AY} = 0$ in Equation 2.4. A verification of the calculation yielding the reproduction number $\mathcal{R}_0$ given by Equation 2.4 is provided in the electronic supplementary material.

The reproduction number $\mathcal{R}_0$ shown in Equation 1 in the manuscript arising from our model admits a natural biological interpretation. To guide this discussion, it is pertinent to refer to the original epidemic model proposed by W. O. Kermack and A. G. McKendrick in 1927 [49], see Figure 2.7-6 below. The corresponding dynamical system is given by

$$\begin{cases}\dot{S} = -\beta\frac{I}{N}S, \\ \dot{I} = \beta\frac{I}{N}S-\omega I, \\ \dot{R} = \omega I.\end{cases} \tag{2.5}$$

Epidemiologically speaking, the basic reproduction number is the average number of secondary infections generated by a single infection in a completely susceptible population. It is proportional to the product of infection/contact ($a$), contact/time ($b$) and time/infection ($c$). The quantity $a$ is the infection probability between susceptible and infectious individuals, $b$ is the mean contact rate between susceptible and infectious individuals and $c$ is the mean duration of the infectious period.

The case of an increasing infected sub-population corresponds to the occurrence of an epidemic. This happens provided that $\dot{I} = \beta\frac{I}{N}S-\omega I > 0$ or $\frac{\beta}{\omega}\frac{S}{N} > 1$. Under the assumption that in the beginning of an epidemic, virtually the total population is susceptible, that is $\frac{S}{N} \approx 1$. As a result, we arrive at the following equivalent condition

$$\mathcal{R}_0 := \frac{\beta}{\omega} > 1.$$

The parameter $\beta$ in Figure 2.7-6 is equal to $ab$ and $\omega$ is equal to $c^{-1}$. This combination of parameters stands to reason as it is a ratio of the effective contact rate $\beta$ and the mean infectious period $\omega^{-1}$.

Since the disease-induced death rate $\delta \approx 0$, the reproduction number in Equation 2 in the manuscript for our model has a similar natural interpretation as the sum of ratios consisting of the effective contact rates $\beta_Y$, $\beta_A$ and mean infectious periods $\lambda_{YR}^{-1}$, $\lambda_{AR}^{-1}$ for the symptomatic and asymptomatic sub-populations, weighted with the probabilities of becoming symptomatic $(1-\alpha)$ or asymptomatic $\alpha$ upon infection.

The effective reproduction number $\mathcal{R}_0(t)$ takes into consideration the susceptibility of the population,

$$\mathcal{R}_0(t) := \frac{\mathcal{R}_0}{N(t)} S(t). \tag{2.6}$$

It is defined to be the average number of secondary cases generated by a typical case. A decrease in the susceptible population overtime will cause a corresponding decrease in the values of the reproduction number. It directly follows by Equation 2.6 that $\mathcal{R}_0(0) = \mathcal{R}_0$, as initially the total human population is assumed to be susceptible. The plot of $\mathcal{R}_0(t)$ is similar to the plot of the susceptible portion, featured in Figure 3 in the manuscript. This is reasonable since Equation 2.6 implies that $\mathcal{R}_0(t)$ is proportional to $S(t)$. Since $\delta \approx 0$, the total population $N(t)$ varies little within a tight envelope around the initial susceptible population $S(0)$. This is easily observable upon inspection of the dynamical system given by Equation 1 in the manuscript, as it is clear that

$$N(t) = S(0) - \delta \int_0^t Y(\zeta) d\zeta.$$

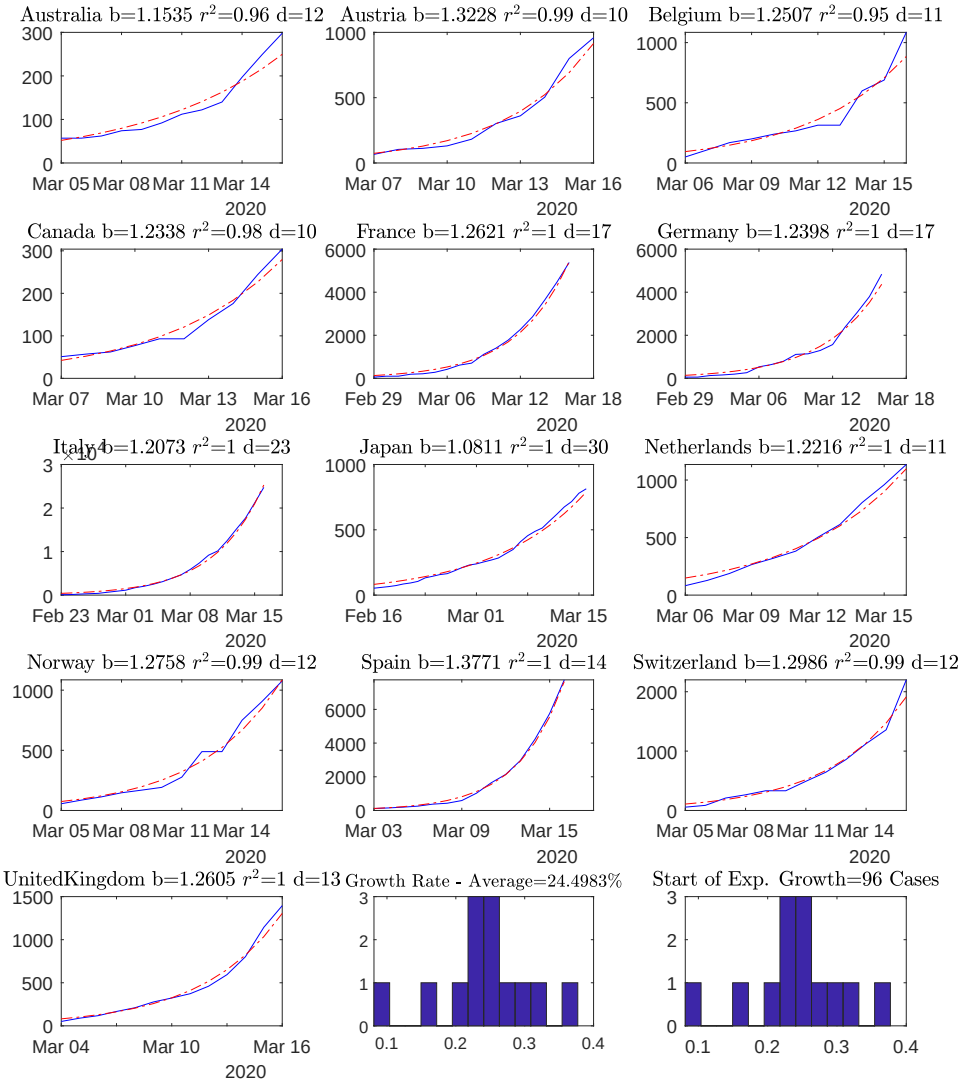


Figure 2.3-2: First three weeks (or less) of data for thirteen countries with COVID-19 cases and strong surveillance systems for communicable diseases.

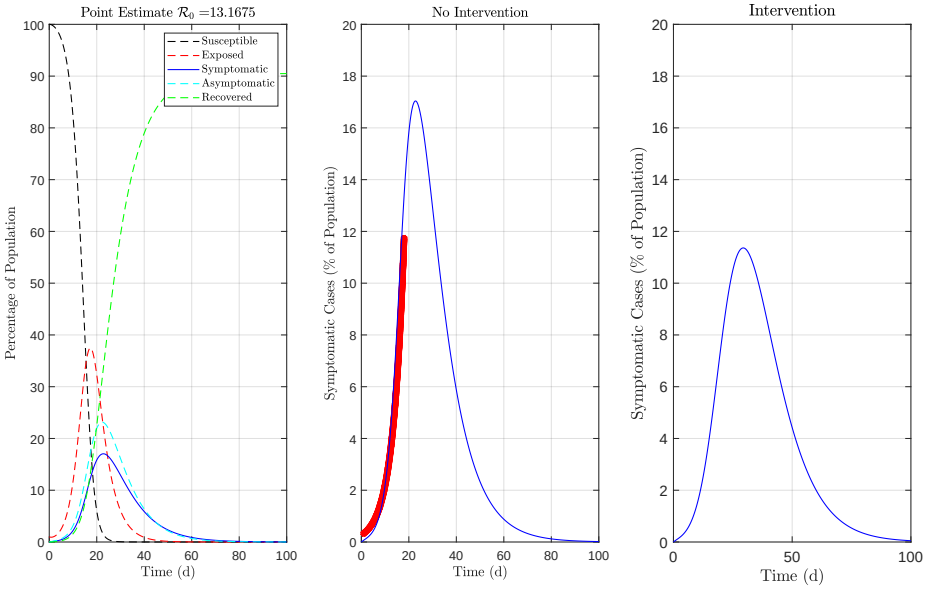


Figure 2.4-3: Numerical implementation of a SEYAR model with the parameters listed on Table 2.1. The left-most panel shows the time series corresponding to a point estimate of $\mathcal{R}_0 = 13.2$. The center panel shows a times series of the symptomatic compartment; the red dots represent the exponential function whose parameters are the average of the thirteen countries studied. The right-most panel shows a simulation representing the effect of limiting contact between the susceptible and infected populations.

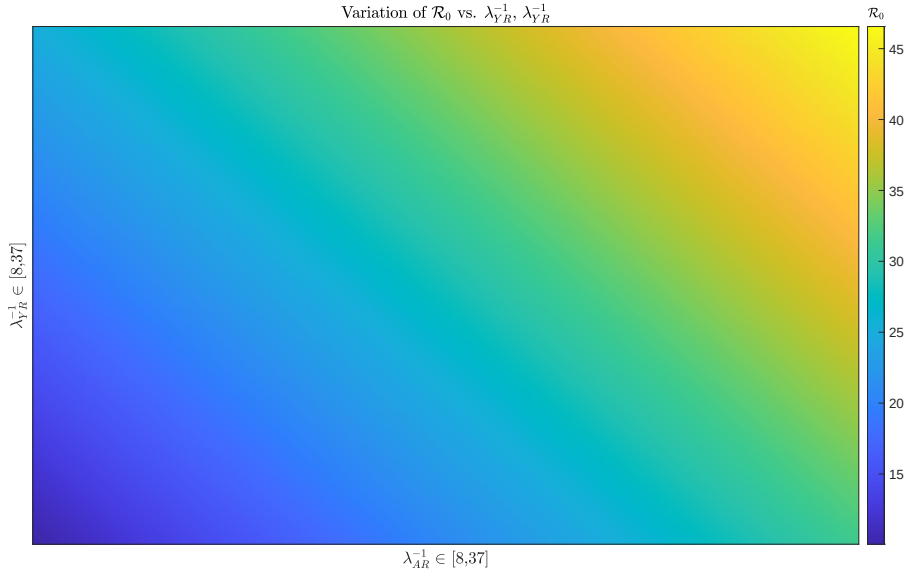


Figure 2.4-4: Heat map showing the variation of the basic reproduction number $\mathcal{R}_0$ with respect to the asymptomatic and symptomatic infectious periods $\lambda_{AR}^{-1}$ and $\lambda_{YR}^{-1}$, respectively.

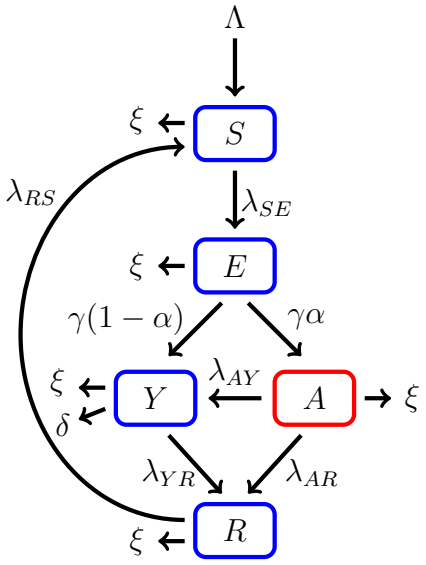


Figure 2.7-5: This figure is a schematic diagram of a generalized COVID-19 model including an asymptomatic compartment. The longer arrows represent progression from one compartment to the next. Hosts enter the susceptible compartment either through birth of migration and then progress through each additional compartment subject to the rates described above.

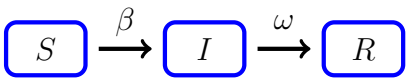


Figure 2.7-6: This figure is a schematic diagram of a $SIR$ model consisted of three compartments, namely: susceptible $(S)$, infected $(I)$ and recovered $(R)$. Humans progress through each compartment subject to the rates described above.

UTSA

# Bibliography


[1] J. M. Read, J. R. Bridgen, D. A. Cummings, A. Ho, C. P. Jewell, *medRxiv* (2020).

[2] T. Liu, *et al.*, *SSRN* (2020).

[3] M. Majumder, K. D. Mandl, *China (January 23, 2020)* (2020).

[4] Z. Cao, *et al.*, *medRxiv* (2020).

[5] S. Zhao, *et al.*, *International Journal of Infectious Diseases* **92**, 214 (2020).

[6] N. Imai, *et al.*, *Reference Source* (2020).

[7] W.-j. Guan, *et al.*, *New England Journal of Medicine* (2020).

[8] World Health Organization, Coronavirus disease (covid-19) outbreak.

[9] World Health Organization, who director-general's opening remarks at the media briefing on covid-19 - 11 march 2020.

[10] K. Mizumoto, K. Kagaya, A. Zarebski, G. Chowell, *Eurosurveillance* **25** (2020).

[11] Z. Hu, *et al.*, *Science China Life Sciences* pp. 1–6 (2020).

[12] L. Zou, *et al.*, *New England Journal of Medicine* (2020).

[13] C. R. MacIntyre, *Global Biosecurity* **1** (2020).

[14] S. Sanche, *et al.*, *Emerging infectious diseases* **26** (2020).

[15] P. Wu, *et al.*, *Eurosurveillance* **25** (2020).

[16] S. Zhang, *et al.*, *International Journal of Infectious Diseases* (2020).

[17] R. Li, *et al.*, *medRxiv* (2020).

[18] Y. Liu, A. A. Gayle, A. Wilder-Smith, J. Rocklöv, *Journal of travel medicine* (2020).

[19] P. L. Delamater, E. J. Street, T. F. Leslie, Y. T. Yang, K. H. Jacobsen, *Emerging infectious diseases* **25**, 1 (2019).

[20] H. Nishiura, G. Chowell, M. Safan, C. Castillo-Chavez, *Theoretical Biology and Medical Modelling* **7**, 1 (2010).

[21] R. Anderson, G. Medley, R. May, A. Johnson, *Mathematical Medicine and Biology: a Journal of the IMA* **3**, 229 (1986).

[22] J. C. Lagarias, J. A. Reeds, M. H. Wright, P. E. Wright, *SIAM Journal on optimization* **9**, 112 (1998).

[23] G. Chowell, C. Viboud, *Infectious disease modelling* **1**, 71 (2016).

[24] G. Chowell, L. Sattenspiel, S. Bansal, C. Viboud, *Physics of life reviews* **18**, 114 (2016).

[25] G. Chowell, C. Viboud, L. Simonsen, S. M. Moghadas, *Journal of The Royal Society Interface* **13**, 20160659 (2016).

[26] C. C.-. R. Team, *MMWR Morb Mortal Wkly Rep* **69**, 343 (2020).

[27] R. M. Anderson, *et al.*, *Philosophical Transactions of the Royal Society of London. Series B: Biological Sciences* **359**, 1091 (2004).

[28] S. A. Lauer, *et al.*, *Annals of Internal Medicine* (2020).

[29] Q. Li, *et al.*, *New England Journal of Medicine* (2020).

[30] J. A. Backer, D. Klinkenberg, J. Wallinga, *Eurosurveillance* **25** (2020).

[31] J. Zhang, *et al.*, *The Lancet Infectious Diseases* (2020).

[32] S. A. Lauer, *et al.*, *medRxiv* (2020).

[33] M. Ki, *et al.*, *Epidemiology and health* p. e2020007 (2020).

[34] N. M. Linton, *et al.*, *Journal of clinical medicine* **9**, 538 (2020).

[35] E. Java, S. Fox, L. A. M. Meyers, *medRxiv* (2020).

[36] R. Li, *et al.*, *Science* (2020).

[37] N. Ferguson, D. Laydon, G. Nedjati-Gilani, *et al.*, Impact of non-pharmaceutical interventions (npis) to reduce covid-19 mortality and healthcare demand. imperial college covid-19 response team (2020).

[38] M. Day, Covid-19: Identifying and isolating asymptomatic people helped eliminate virus in italian village (2020).

[39] W. H. Organization, *et al.* (2020).

[40] H. Nishiura, *et al.*, *medRxiv* (2020).

[41] H. Nishiura, *et al.*, The rate of underascertainment of novel coronavirus (2019-ncov) infection: Estimation using japanese passengers data on evacuation flights (2020).

[42] M. Day, Covid-19: Four fifths of cases are asymptomatic, china figures indicate (2020).

[43] R. Wölfel, *et al.*, *Nature* pp. 1–10 (2020).

[44] A. J. Kucharski, *et al.*, *The lancet infectious diseases* (2020).

[45] F. Zhou, *et al.*, *The Lancet* (2020).

[46] X. He, *et al.*, *medRxiv* (2020).

[47] J. B. Aguilar, J. B. Gutierrez, *Bulletin of Mathematical Biology* **82**, 42 (2020).

[48] P. Van den Driessche, J. Watmough, *Mathematical biosciences* **180**, 29 (2002).

[49] W. Kermack, A. Mckendrick, *Proc Roy Soc London* **A 115**, 700 (1927).